University of Pennsylvania
ScholarlyCommons

Departmental Papers (MSE) | Department of Materials Science & Engineering

April 2004

Biomimetic surfaces via dextran immobilization : grafting density and surface properties

Davide Miksa
University of Pennsylvania

Elizabeth R. Irish
University of Pennsylvania, eirish@seas.upenn.edu

Dwayne Chen
University of Pennsylvania

Russell J. Composto
University of Pennsylvania, composto@lrsm.upenn.edu

David M. Eckmann
University of Pennsylvania, eckmanndm@uphs.upenn.edu

Follow this and additional works at: http://repository.upenn.edu/mse_papers

Recommended Citation

Miksa, D., Irish, E. R., Chen, D., Composto, R. J., & Eckmann, D. M. (2004). Biomimetic surfaces via dextran immobilization : grafting density and surface properties. Retrieved from http://repository.upenn.edu/mse_papers/2

Copyright Materials Research Society. Reprinted from MRS Proceedings Volume 826E.
2004 Spring Meeting Symposium V
Proteins as Materials
Publisher URL: http://www.mrs.org/members/proceedings/spring2004/v/V2_2.pdf

This paper is posted at ScholarlyCommons. http://repository.upenn.edu/mse_papers/2
For more information, please contact libraryrepository@pobox.upenn.edu.

Biomimetic surfaces via dextran immobilization : grafting density and surface properties

Abstract
Biomimetic surfaces were prepared by chemisorption of oxidized dextran (M_w = 110 kDa) onto SiO_2 substrates that were previously modified with aminopropyl-tri-ethoxy silane (APTES). The kinetics of dextran oxidation by sodium metaperiodate ($NaIO_4$) were quantified by ^1H NMR and pH measurements. The extent of oxidation was then used to control the morphology of the biomimetic surface. Oxidation times of 0.5, 1, 2, 4, and 24 hours resulted in <20, ~30, ~40, ~50 and 100% oxidation, respectively. The surfaces were characterized by contact angle analysis and atomic force microscopy (AFM). Surfaces prepared with low oxidation times revealed a more densely packed "brushy" layer when imaged by AFM than those prepared at low oxidation times. Finally, the contact angle data revealed, quite unexpectedly, that the surface with the greatest entropic freedom (0.5 h) wetted the fastest and to the greatest extent ($THETA_{APTES}$ > $THETA_{1h}$ > $THETA_{2,4h}$ > $THETA_{0.5h}$).

Comments
Copyright Materials Research Society. Reprinted from MRS Proceedings Volume 826E.
2004 Spring Meeting Symposium V
Proteins as Materials
Publisher URL: http://www.mrs.org/members/proceedings/spring2004/v/V2_2.pdf

This conference paper is available at ScholarlyCommons: http://repository.upenn.edu/mse_papers/2

Biomimetic Surfaces via Dextran Immobilization: Grafting Density and Surface Properties

Davide Miksa,[1] Elizabeth R. Irish,[2] Dwayne Chen,[1] Russell J. Composto,[2] David M. Eckmann[1]
Departments of [1]Anesthesia and [2]Material Science and Engineering, University of Pennsylvania, Philadelphia, PA 19104

ABSTRACT

Biomimetic surfaces were prepared by chemisorption of oxidized dextran (M_w = 110 kDa) onto SiO_2 substrates that were previously modified with aminopropyl-tri-ethoxy silane (APTES). The kinetics of dextran oxidation by sodium metaperiodate ($NaIO_4$) were quantified by ^1H NMR and pH measurements. The extent of oxidation was then used to control the morphology of the biomimetic surface. Oxidation times of 0.5, 1, 2, 4, and 24 hours resulted in <20, ~30, ~40, ~50 and 100% oxidation, respectively. The surfaces were characterized by contact angle analysis and atomic force microscopy (AFM). Surfaces prepared with low oxidation times revealed a more densely packed "brushy" layer when imaged by AFM than those prepared at low oxidation times. Finally, the contact angle data revealed, quite unexpectedly, that the surface with the greatest entropic freedom (0.5 h) wetted the fastest and to the greatest extent ($\theta_{APTES}>\theta_{1h}>\theta_{2,4h}>\theta_{0.5h}$).

INTRODUCTION

Evermore pressing needs to control the biochemical interactions at the tissue/material interface have prompted scientist to consider polysaccharides and proteoglycans, which are native to the cellular glcocalyx,[1] as coatings for biomaterials.[2-4] Although different aspects of such coatings have been studied in the past, the wettability and spatial organization at the biomaterial surface are still recognized as the limiting factors in biocompatibility. It is therefore essential to develop surface synthetic techniques that will afford reproducible control over the surface morphology of the biomaterial coating. Furthermore, it is imperative to characterize those surfaces with the necessary resolution and under conditions that are relatable to their proposed working environment so that their performance can be directly attributed to their structural and functional properties. It has, therefore, been the goal of the present study to create dextran coated surfaces having varying grafting density between dextran and the substrate. Since increased surface roughness can promote protein adhesive as well as micro-embolic events, smooth silicon wafers with a SiO_2 surface layer were chosen as the starting point for further modification. The well established chemistry of organo-silane self-assembled monolayers (SAMs)[5] afforded an amine functionalized SiO_2 surface onto which dextran was immobilized via reductive amination. Although there are several techniques that allow surface characterization at the molecular level, the authors have focused on atomic force microscopy (AFM) and H_2O contact angle as the primary modes of analysis. AFM also offered the possibility to conduct force of adhesion measurements, which provided further insight in the dextran-substratum, and dextran-probe interactions.

EXPERIMENTAL

Materials.

All reagents and solvents were used as received unless otherwise stated. Aminopropyltriethoxysilane (APTES), sodium periodate, 99% ($NaIO_4$), sodium cyanoborohydrate ($NaBH_3CN$), and dimethylformamide were purchased from Sigma-Aldrich Co. Dextran from Leuconostoc ssp (Mw = 110,000, Mw/Mn = 1.52) was supplied by Fluka Chemie. Deuterium oxide (D_2O, 99.9%) for ^1H NMR measurements was obtained from Cambridge Isotope Laboratories, Inc. H_2SO_4 (96% by assay) and H_2O_2 (30% by assay) were obtained from Fisher Scientific. Finally, silicon wafers (<1-0-0>, R = 1-5 Ω cm,) were purchased from Silicon Quest Int'l (Santa Clara, CA). All experiments made use of water that was treated with a Millipore® filtration system so that the resistivity of the water measured 18.2 mΩ.

APTES surface preparation

Silicon surfaces (3.0 cm x 4.5 cm) were etched clean by immersion in "piranha" solution (70% H_2SO_4 and 30% H_2O_2, v/v) for 20 min. at 80 °C. The surfaces were then washed with copious amounts of water and allowed to soak in water overnight. Afterwards, the surfaces were blow dried with compressed $N_{2(g)}$ and exposed to ultra violet light in a UVO-Cleaner model 144A (Jelight Company Inc.; Irvine, CA) for 20 min. This cleaning procedure afforded a homogeneous silanol layer as the starting point for further surface modifications. The silicon surfaces were then functionalized with an APTES self-assembled monolayer (SAM) by vapor deposition under inert atmosphere as afforded by a glove-box. A 9 cm high, 7 cm diameter screw cap glass jar was chosen as the reaction vessel for the APTES vapor deposition. 2 mL of APTES were transferred into the jar by means of a graduated syringe. A freshly cleaned and UV treated silicon surface was then laid face down on a 2 cm high glass ring that was placed inside the jar. The ring functioned as a platform ensuring that the surface was equidistant from the APTES. The jar was then sealed with Parafilm® and heated at 80 °C for 1 hour outside the glove-box. At these conditions the reactive side of the silicon surface was exposed to an APTES vapor pressure of 4.01 Torr.[6]

Dextran surface immobilization

The validity of $NaIO_4$ oxidation of various carbohydrates has long been established.[2;7] The present work involved manipulation of the $NaIO_4$ oxidation of dextran in order to control the extent of "brushiness" (*i.e.* grafting density) of the biomimetic coating. A brief summary of the chemistry follows. The oxidation of the anhydroglucopyranoside (**1**) (see Figure 1) subunits by $NaIO_4$ afforded the dialdehyde described by (**2**) as well as formic acid. The reaction proceeded via the formation of two subsequent cyclic periodate esters and therefore necessitated two moles of $NaIO_4$ per mole of (**1**). The first of such esters was formed by the nucleophilic attack of the vicinal hydroxyls of carbons C2, C3, or C4 on the iodine of the first IO_4^-. The crucial part at this stage of the mechanism was the bond breaking between the hydroxyl bearing carbons. This first bond cleavage resulted in the formation of a dialdehyde that is one carbon longer than (**2**) and still has a hydroxyl group left. The second cyclic periodate ester was formed by the nucleophilic

attack of the remaining hydroxyl and one of the aldehyde oxygens. The subsequent C-C bond cleavage afforded the final dialdehyde, (**2**), and formic acid. Finally, (**2**), which is in equilibrium with its cyclic hydrate (**3**), underwent a reductive amination when incubated with APTES modified substrates in the presence of $NaBH_3CN$. This resulted in stable covalent bonds between the dextran and the SiO_2. The extent of dextran oxidation was quantified by means of ^1H NMR spectroscopy (Bruker, 250 MHz) *in situ* monitoring of HCO_2H production. The NMR results were also confirmed by pH measurements and are summarized in Figure 2, which shows the calculated concentrations of dextran, $NaIO_4^-$, and HCO_2H. Also shown in Figure 2 is the dextran oxidation profile which initially increases rapidly, and after ~10 h asymptotically approaches 70%.

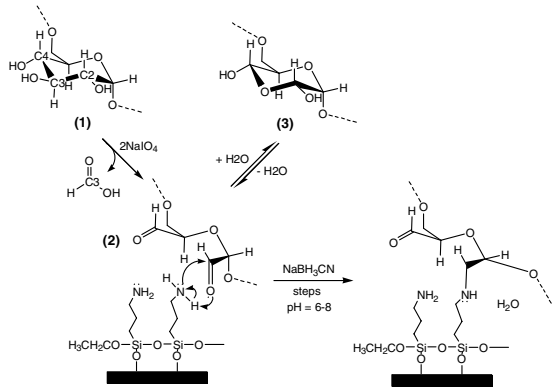

Figure 1. Oxidation of glucopyranoside subunits by $NaIO_4$ with formation of HCO_2H, and subsequent surface immobilization via reductive amination.

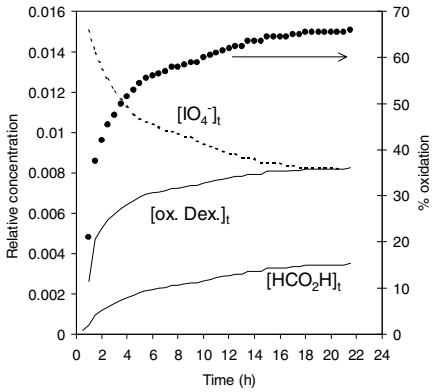

Figure 2. Calculated concentration profiles for the oxidation of dextran by $NaIO_4$, as well as the co-production of HCO_2H. The corresponding % oxidation of dextran is also indicated.

<u>Atomic force microscopy</u>

All imaging scans (tapping mode) as well as force of adhesion (F_{adh}) measurements were performed with a DI Multimode AFM scanning probe microscope (Veeco Metrology, Chadds Ford, PA). A liquid cell in conjunction with Si_3N_4 tips (spring constant = 0.06 N/m for imaging, 0.32 N/m for force measurements) were employed for scans under aqueous conditions. The tips were cleaned by brief immersion in "piranha" solution followed by rinsing with copious amounts of water. The tips were then allowed to dry in air and were then exposed to UV-light, as per manufacturer's suggestion, for 15 minutes. Imaging scans were acquired at 4 μm/s (10 x 10 μm^2) and 2 μm/s (1 x 1 μm^2). Furthermore, image optimization was achieved by increasing

the amplitude set-point until the probe was fully retracted. Then, the set-point was reduced in small increments until the probe re-engaged the surface. This procedure ensured minimization of tip-sample forces, and therefore any tip induced perturbation of the surface was also minimized. Force of adhesion measurements were performed in contact mode also under aqueous conditions. The scan size was set to zero prior to engaging the tip to the surface. All force of adhesion measurements herein reported were collected with the same probe using identical microscope settings. The scan rate was 0.5 Hz, and the scan length was 1.0 μm,. The force curves were collected in continuous mode. When the probe/surface interaction had reached equilibrium, and the force profile remained unchanged while in continuous mode, a minimum of five curves per region were collected on five different areas of the sample.

Contact angle

Time dependant advancing and receding H_2O contact angle measurements were performed at room conditions with a Ramé-Hart (Mountain Lakes, NJ) model 100-00 goniometer equipped with a software controlled auto-pipeting system and the DROPimage advanced software package. The corresponding contact angle data was afforded by a numerical curve fit of the droplet profile at the three-phase boundary as captured by a CCD camera.

RESULTS AND DISCUSSION

In order to investigate the effect that varying dextran grafting density (*i.e.* varying oxidation time) had on surface wetting, the change in contact angle (C.A.) of a 1 μL H_2O drop was recorded every five seconds over one minute on all surfaces. The data are summarized in Figure 3 (left), which shows the result of measurements of at least three different 1 μL drops corresponding to three different regions on any given surface. Due to the complete wetting (contact angle less than 5°) on the SiO_2 and the 24 h dextran surfaces their corresponding contact angles are not shown. In order to avoid complications due to evaporation, no data was collected after 60 s. These relaxation measurements allowed the extent as well as the rate of wetting, k_W s^{-1} (Table 1), of the different surfaces to be considered. A comparison of the grafting density with the extent of wetting ($\theta_{APTES}>\theta_{1h}>\theta_{2,4h}>\theta_{0.5h}$), or k_W did not yield any systematic correlation. Nevertheless, the surface modified with 0.5 h oxidized dextran (lowest grafting density) repeatedly exhibited the largest extent and the fastest rate of wetting. This observation is counterintuitive since the surface with the lowest grafting density of dextran should also have the largest surface entropy and should, therefore, undergo the largest structural rearrangement upon hydration. It was, therefore, initially thought that the 0.5 h oxidized dextran surfaces would exhibit the slowest rate of wetting. In order to elucidate the morphology of the dextranized surfaces further, advancing/receding measurements were also conducted (Figure 3, right). These measurements were collected every five seconds over a 65 second interval. Furthermore, it is important to note that after each advancing and receding step a five second relaxation period was allowed for prior to the next volume change (see volume profile). The advancing/receding data offer a qualitative measure of the homogeneity of the dextranized surfaces. In fact, the advancing sides of the plots show little variation as the droplet volumes, and therefore areas, increase from 2 to 5 μL (4.3-8.6 mm^2).

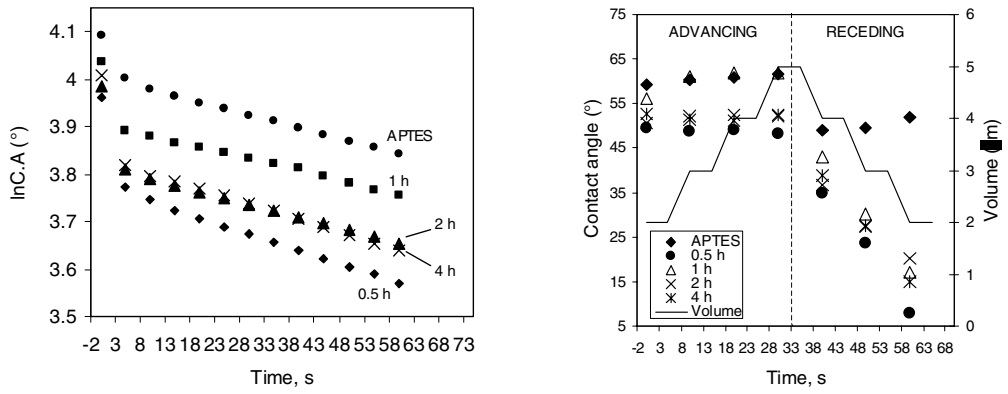

Figure 3. Plot of the natural log of H_2O contact angle versus time (left), and advancing and receding contact angle measurements (right) for dextranized surfaces.

The hysteresis between the advancing and receding measurements did not reflect the differences in extent of conformational change that the various dextranized surfaces are thought to undergo upon hydration. This is consistent with the relaxation data. As expected, however, the receding contact angle was substantially smaller than the advancing. This has been explained by Andrade[8] and by Holly et al.[9] who pointed out that, once hydrated, polymer chains achieve conformations that minimize the interfacial tension. The morphology of the different surfaces was further studied under aqueous conditions by atomic force microscopy (AFM). The imaging scans afforded the measurement of the surface roughness (Figure 4.), and also gave a visual measure of the extent of grafting density (*i.e.* "brushiness") for the individual dextran surfaces. Not shown in Figure 4 is the 24 h dextran surface. This was a particularly thick surface (see Table 1), and therefore was considered separately.

Table 1. Ellipsometric thickness, rate of wetting and force of adhesion for specified surfaces

SURFACE	THICKNESS (Å)[a]	k_W x 10^3, (sec^{-1})	F_{adh} (nN)[b]
SiO_2	20.7 ± 0.58[c]	NA	0
APTES	5.00 ± 1.15	2.81	2.90 ± 0.58
0.5 h Dextran	4.67 ± 3.06	3.54	2.41 ± 0.53
1.0 h Dextran	3.00 ± 2.08	2.47	1.74 ± 0.51
2.0 h Dextran	2.33 ± 1.00	2.75	5.00 ± 1.46
4.0 h Dextran	2.33 ± 1.73	3.23	2.23 ± 0.46
24.0 h Dextran	973 ± 16.8	NA	NA

[a]Dry; [b]Aqueous; [c]Baseline

As can be seen from Figure 4, the roughness of the dextran surfaces decreased in the 0.5 – 2.0 h range, therefore decreasing with increasing grafting density. The 4.0 h surface, however, exhibited a roughness similar to that of the 0.5 h surface. This is possibly due to the fact that in the 2.0 - 4.0 h range dextran layers start overlapping which results in an increase in roughness.

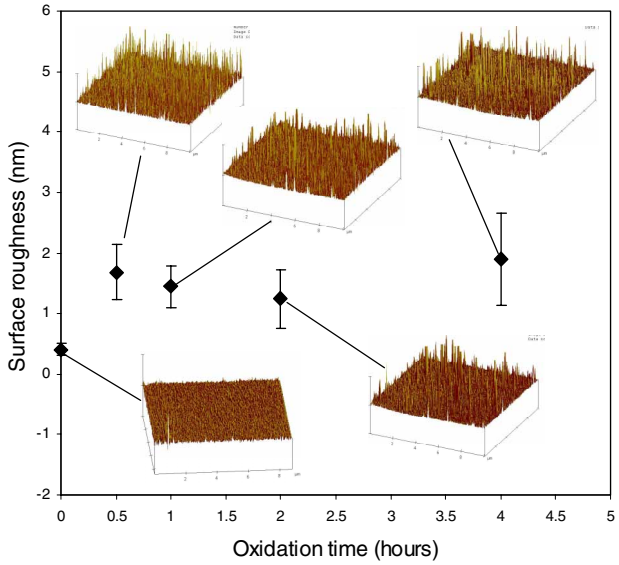

Figure 4. Root-mean-square surface roughness as a function of oxidation time for 0.5 – 4.0 h dextran surfaces under aqueous conditions (10 μm scans). Z scale is 20 nm.

The extent of deflection undergone by the Si_3N_4 probe upon approach toward and retraction from the above mentioned surfaces was also measured by AFM. The corresponding force of adhesion (F_{adh}, nN) values are summarized in Table 1. With the exception of the 2.0 h surface, the trend in F_{adh} seems to follow that of the surface roughness. The unusually large deflection measured in the case of the 2.0 h surface is most likely due to multiple adhesion events, as evidenced by the force plots (data not shown). Also shown in Table 1 are the dry ellipsometric thickness values for all surfaces. Although informative, they should not be considered in an absolute sense. Thickness measurements based on light polarization changes (*i.e.* ellipsometry) are best suited for surfaces that are continuous (constant refractive index). As shown by the AFM scans in Figure 4, the dextranized surfaces are certainly not continuous. Moreover, the ellipsometer used in our research had a "reading" area of ~1 mm^2. Therefore, the ellipsometry data should be considered with respect to the density of dextran "bristles" per surface. In that regard, the areal density of dextran decreases with increasing oxidation time, as expected.

CONCLUSION

Dextranized surfaces having varying grafting densities were prepared by controlling the duration of the $NaIO_4$ oxidation, a generally accepted functionalization method. They were characterized in an effort to correlate wettability, roughness, and contact force to surface morphology. It is the opinion of the authors that the present data warrants further investigations in the affinity that these surfaces might exhibit toward serum proteins.

ACKNOWLEDGMENT

The authors are grateful for the financial support provided by the following grants: NIH R01 HL60230, R01 67986 and T32 GM07612.

REFERENCES

(1) Cryer, A. *Biochemical Interactions at the Endothelium*; Elsevier: New York, 1983; pp 5-30.
(2) Dai, L.; St John, H. A. W.; Bi, J.; Zientek, P.; Chatelier, R. C. *Surf.Inter.Analy.* 2000, *29*, 46-55.
(3) Hartley, P. G.; McArthur, S. L.; McLean, K. M.; Griesser, H. J. *Langmuir* 2002, *18*, 2483-2494.
(4) Mason, M.; Vercruysse, K. P.; Kirker, K. R.; Frisch, R.; Marecak, D. M.; Prestwich, G. D.; Pitt, W. G. *Biomaterials* 2000, *21*, 31-36.
(5) Elender, G.; Kuhner, M.; Sackmann, E. *Biosensors & Bioelectronics* 1996, *11*, 565-577.
(6) Ditsent, V. E.; Skorokhodov, I. I.; Terenteva, N. A.; Zolotarev, M. N.; Belyakova, Z. V.; Belikova, Z. V. *Zhu.Fizi.Khim.* 1976, *50*, 1905-1906.
(7) Hughes, G.; Nevell, T. P. *Tran.Farad.Soc.* 1948, *44*, 941-948.
(8) Andrade J.D. *Poly.Sci.Tech.* 1986, *34*, 29-40.
(9) Holly F.J.; Refojo M.F. *J.Biomed.Mate.Rese.* 1975, 9, 315-326.